Proceedings of the Estonian Academy of Sciences,
2020, **69**, 1, 74–80
https://doi.org/10.3176/proc.2020.1.08
Available online at www.eap.ee/proceedings

Dual coherent light array model for reflective rectangular metallic grating

Xiangnan Qiao, Jinkui Chu*, and Ran Zhang

School of Mechanical Engineering, Dalian University of Technology, Linggong Road, Ganjingzi District, 116024 Dalian, Liaoning Province, China

Received 4 November 2019, accepted 3 December 2019, available online 17 February 2020

Abstract. To study the mechanism of periodic change of reflective rectangular metallic gratings' diffraction efficiencies, a dual secondary coherent light source array model was established based on the theory of Fabry-Pérot resonator. It was assumed that when incident light falls on the grating surface, it transforms into two coherent sources on each grating period. One is on the upper surface of the grating, reflected by the metal surface; the other is at the entrance of the grating groove and propagates in the form of a fundamental mode (λ_f). Based on the above mentioned hypothesis, formulae for the phase difference $\Delta\phi$ of two sources and diffraction efficiency for the first and zero order with grating height h, were established. $\Delta\phi$ and h are linear relationships, the phase difference $\Delta\phi$ change due to the change of grating height h is the essencial cause of periodic changes of the diffraction efficiencies. When $\Delta\phi$ has a certain value, the energy is distributed only in the zero or the first order direction. The model does not only show the change regularity of each diffraction order's diffraction efficiency of reflective rectangular metallic grating, but it also shows the correlation of each diffraction order. It can help to predict diffraction performance of rectangular metallic gratings and to design gratings.

Key words: Fabry-Pérot resonator, dual secondary coherent light source array model, fundamental mode, phase difference, diffraction efficiency.

1. INTRODUCTION

Grating is widely used in optical field due to its periodic structure, diffraction and polarization characteristics. In 1998, Ebbesen et al. discovered the phenomenon of ultra-transmission of hole array with diameter smaller than the length of incident light. They believed that the ultra-transmission phenomenon is caused by the coupling of surface plasmon and incident light on hole array [1]. At present, researches on diffraction grating phenomenon with feature size smaller than incident light's wavelength mainly focus on two theories: surface plasmon resonance and Fabry-Pérot (FP)-like resonance. Porto et al. studied the diffraction phenomenon of resonant waveguide gratings and surface plasmon resonance theory, respectively [2]. D'Aguanno et al. believed that both surface plasmon and FP-like resonance can affect the diffraction grating, and that FP-like resonance supported by the waveguide mode in each slit of the grating played a leading role [3], especially under the condition where the incident light is perpendicular to the grating surface and there is no prism or substrate. Astilean et al. studied the distribution of energy in the grating grooves during diffraction process. They found that the energy in the

* Corresponding author, chujk@dlut.edu.cn

grooves exhibited a periodic distribution in the direction of grating height. Then they considered the groove of the grating as a FP-like resonator [4]. For a long time, scholars have been studying the influence of FP-like resonance on transmission or reflective grating diffraction, and gradually confirmed the leading role of FP-like resonance [5–9]. Reflective grating is often used to measure displacement. The grating displacement measurement system converges diffraction lights together to generate the interference signal [10–15]. Moharam et al., founders of rigorous coupled-wave analysis (RCWA) [16–19] calculated the diffraction of the reflective metallic grating. The grating period has the same magnitude as the wavelength of the incident light. They described the trend of the periodic change of the zero and the first order diffraction efficiency dependence on the grating height (note that one of the zero and the first order goes up and the other one goes down, and vice versa [19]). For reflective rectangular metallic gratings, the reason and the essence of such a regularity should be further studied and discussed. Furthermore, a model is required to not only study the change regularity of energy in a single grating period or groove, but also relate them to the diffraction of the grating.

A dual secondary coherent light source array model was established based on the theory of FP resonator to study the diffraction mechanism of reflective rectangular metallic grating with subwavelength feature size. In this paper, the surfaces of the grating ridges and grooves illuminated by the incident light are considered as two kinds of secondary coherent light sources. The source on grating ridges is reflected by the metal surface. The source on grating grooves propagates in grooves as fundamental mode [3]. The phase difference between two sources depends on the fundamental mode's propagation distance in grooves. The model was used to reflect the relationship between grating height; and the zero and the first order diffraction efficiency. The diffraction process is affected not only by FP-like resonance, but also by the reflected light from the upper surface of the grating. The mechanism of how grating height affects diffraction of reflective rectangular metallic grating was further analysed. In addition, the intrinsic link between the zero and the first order diffraction efficiency was discussed.

2. MODEL OF DUAL SECONDARY COHERENT LIGHT SOURCE ARRAY

In this section, the dual secondary coherent light source array model was established based on the theory of Fabry-Pérot resonance. The environment was set up at the beginning. The grating period had similar size as the wavelength of incident light; and the size of grating groove was smaller than the wavelength of the incident light.

Figure 1 describes the dual light source array model in more detail. Inspired by Fraunhofer diffraction theory [20], but different from it, each period of the reflective rectangular metallic grating is composed of a ridge and a groove. The ridge and groove surfaces covered by the incident light were considered as two secondary coherent light sources. As shown in Fig. 1, the ridge surface is called secondary light source 1, and the groove surface is called secondary light source 2. When the incident light enters into the grating groove, energy transforms into fundamental mode modulated by the grating. Then, the fundamental mode is reflected from the bottom of the groove and propagated to the upper surface of the grating. Finally, the

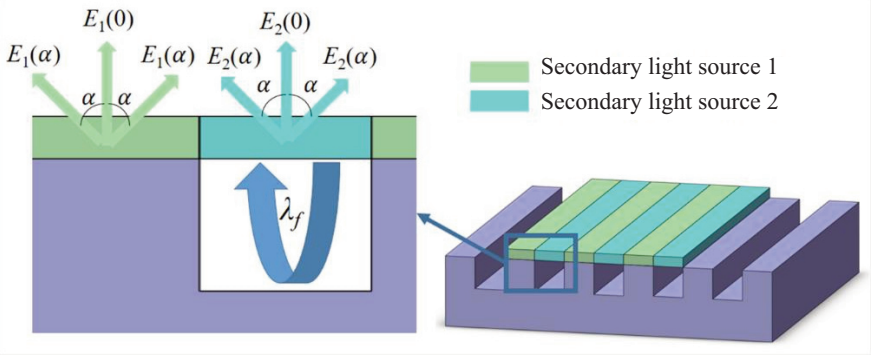

Fig. 1. Dual light source array model for metallic grating.

fundamental mode transforms into the propagation light with the same wavelength as of incident light. Two kinds of coherent secondary light sources are composed of two kinds of coherent secondary light source arrays, and are alternatively arranged on the upper surface of the grating.

As shown in Fig. 1, the periodic structure or the grating consists of resonant cavities, which are parallel to each other with the grating period d [4–8]. If incident light is perpendicular to the grating, it will be modulated by the grating. Then, a part of the energy of the incident light propagates in grating grooves in the form of fundamental mode. The wavelength λ_f of fundamental mode is determined by the grating material, grating groove filling medium, groove width, and the wavelength of incident light [7].

The dual secondary coherent source array model was briefly described above. More detailed description of the model will be described below.

As shown in Fig. 1, the interval between any two coterminous centres of secondary light sources under arbitrary fill factor f is d/2. Inspired by the Fraunhofer's diffraction theory, the electric field strength E(α) in any direction can be expressed as follows:

$$\begin{aligned} \mathrm{E}(\alpha) &= \mathrm{E}_1(\alpha) e^{-\mathrm{i}(\omega t+\phi_1)} \sum_{n=0}^{N-1} e^{-\mathrm{i}knd\sin(\alpha)} + \mathrm{E}_2(\alpha) e^{-\mathrm{i}(\omega t+\phi_2)} \sum_{n=0}^{N-1} e^{-\mathrm{i}k(2n+1)d\sin(\alpha)/2} \\ &= \left(E_1(\alpha) \mathrm{e}^{-i(\omega t+\phi_1)} + E_2(\alpha) \mathrm{e}^{-i(\omega t+kd\sin(\alpha)/2+\phi_2)} \right) \left(1-\mathrm{e}^{-iNkd\sin(\alpha)}\right) \Big/ \left(1-\mathrm{e}^{-ikd\sin(\alpha)}\right), \end{aligned} \tag{1}$$

where α represents both positive and negative angles; $E_1(\alpha)$ and $E_2(\alpha)$ represent the electric amplitude functions of the secondary light source 1 and the secondary light source 2 in α direction; ϕ_1 and ϕ_2 represent the initial phase of the secondary light source 1 and the secondary light source 2, respectively; ω represents the angular frequency of the incident light; N represents the number of the grating period covered by the incident light. All the above mentioned electric amplitudes are unknown functions determined mainly by the same parameters that determined λ_f, here $E_1(\alpha)$ and $E_2(\alpha)$ stay constant at the grating height h. By adding $k = 2\pi/\lambda$ and $\sin(\theta) = \lambda/d$ in Eq. (1), the electric amplitude vectors E(α) in the first and zero order directions can be expressed as follows:

$$\mathrm{E}(\theta) = \left(\mathrm{E}_1(\theta) e^{-\mathrm{i}(\omega t+\phi_1)} + \mathrm{E}_2(\theta) e^{-\mathrm{i}(\omega t+\pi+\phi_2)} \right) \left(1-e^{-2\mathrm{i}N\pi}\right) \Big/ \left(1-e^{-2\mathrm{i}\pi}\right), \tag{2}$$

$$\mathrm{E}(0) = N\mathrm{E}_1(0) e^{-\mathrm{i}(\omega t+\phi_1)} + N\mathrm{E}_2(0) e^{-\mathrm{i}(\omega t+\phi_2)}. \tag{3}$$

Both positive and negative angles of diffraction are considered as θ for convenience, $E_1(\theta)$ and $E_2(\theta)$ are the electric field amplitudes of the secondary light source 1 and the secondary light source 2 in the first order directions, $E_1(0)$ and $E_2(0)$ are the electric field amplitudes of the secondary light source 1 and 2 on zero order direction. Ignoring the term that includes ω, the interference light intensities $I(\theta) = |E(\theta)|^2$ and $I(0) = |E(0)|^2$ of the first and the zero orders can be expressed as follows:

$$\mathrm{I}(\theta) = \left(\mathrm{E}_1^2(\theta) + \mathrm{E}_2^2(\theta) + 2\mathrm{E}_1(\theta)\mathrm{E}_2(\theta)\cos(\Delta\phi - \pi) \right) \left(1-\cos 2N\pi\right) \Big/ \left(1-\cos 2\pi\right), \tag{4}$$

$$\mathrm{I}(0) = \mathrm{E}_1^2(0) + \mathrm{E}_2^2(0) + 2\mathrm{E}_1(0)\mathrm{E}_2(0)\cos(\Delta\phi). \tag{5}$$

$\Delta\phi = \phi_1 - \phi_2$ represents the phase difference of the secondary light source 1 and the secondary light source 2. Equations (4) and (5) show that I(θ) and I(0) are periodic functions on Δϕ under arbitrary N. The term $(1-\cos 2N\pi)/(1-\cos 2\pi)$ of Eq. (4) demonstrates that the interference light intensity reaches to the maximum in the first order direction. Δϕ was assumed to depend only on the distance which the fundamental mode travels in the grooves of the grating, Δϕ can be expressed as follows:

$$\Delta\phi=4\pi h/\lambda_f. \tag{6}$$

For $h=M\lambda_f/2$:

$$I(\theta)=E_1^2(\theta)+E_2^2(\theta)-2E_1(\theta)E_2(\theta), \tag{7}$$

$$I(0)=E_1^2(0)+E_2^2(0)+2E_1(0)E_2(0). \tag{8}$$

For $h = (2M+1)\lambda_f/4$:

$$I(\theta)=E_1^2(\theta)+E_2^2(\theta)+2E_1(\theta)E_2(\theta), \tag{9}$$

$$I(0)=E_1^2(0)+E_2^2(0)-2E_1(0)E_2(0). \tag{10}$$

M stands for arbitrary natural number.

3. DISCUSSION

As shown in Fig. 2, a transverse-magnetic (TM) polarized light (the magnetic field vector parallel to the grooves of the grating) at the wavelength of $\lambda = 532$ nm is modelled to understand the effect of the zero and the first order diffraction efficiencies related to the parameters of the grating. A schematic diagram of the rectangular metallic grating diffraction is depicted in Fig. 2.

Equations (7) and (8) show that the light intensities of the first order reach to the minimum while the zero order reaches to the maximum if $h = M\lambda_f/2$. Equations (9) and (10) show that the light intensities of the first order reach the maximum while the zero order reaches the minimum if $h = (2M+1)\lambda_f/4$. Formulae (4) and (5) show that the diffraction efficiency of the zero and the first order varies periodically, and the peak value and the valley value of the first order overlap with the valley value and peak value of the zero order, respectively.

In order to verify the correctness of the trend obtained by the model presented in this paper, RCWA is adopted to obtain the change diagram of the diffraction efficiency of the first and the zero order diffraction light with the change of grating height h and duty ratio f. Specific parameters are as follows: the TM polarized incident light with the wavelength of 532 nm is perpendicular to the grating; the grating period d composing of alternating regions of ridge and groove are assumed to be 752 nm. The grating with fill factor f from 0 to 1 denotes the proportion of a grating period occupied by a grating ridge, and grating height h

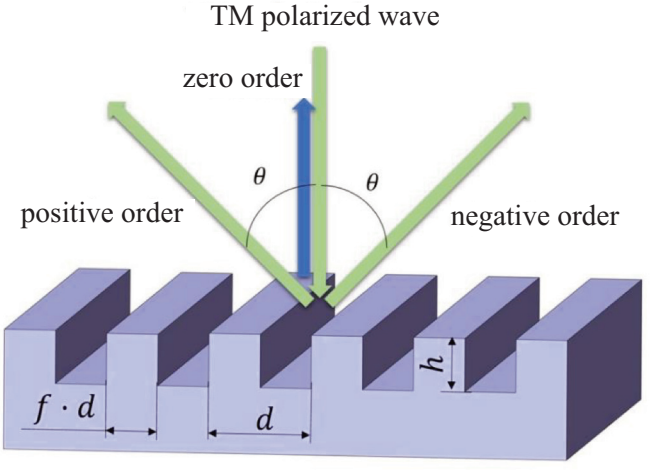

Fig. 2. Geometry of the rectangular metallic grating diffraction.

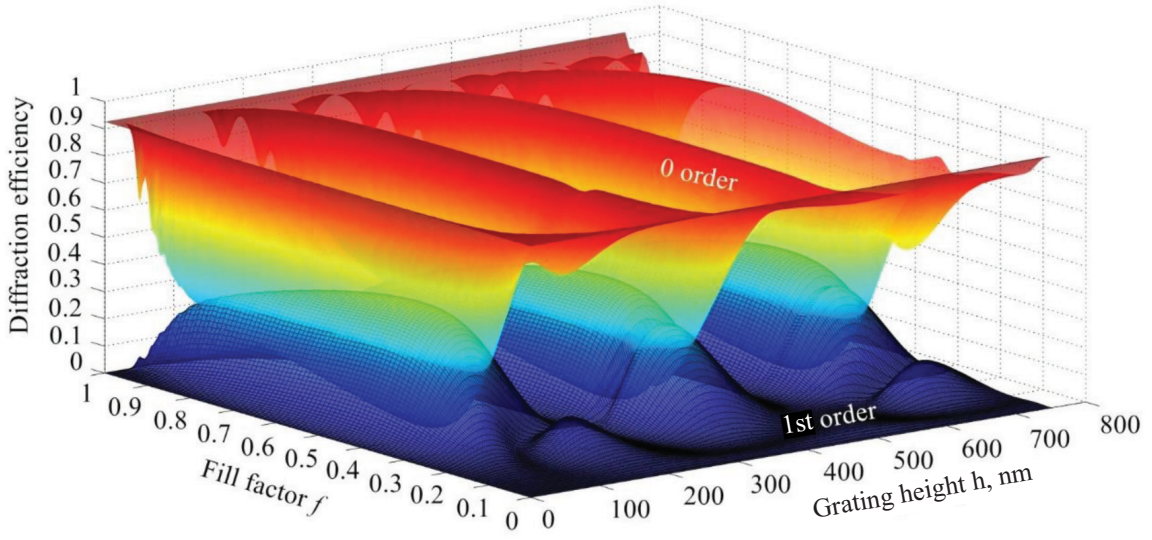

Fig. 3. Diffraction efficiencies of the first and the zero order under TM condition as a function of ridge height h (0–d) and fill factor f (0–1) for aluminium rectangular gratings (d = 752 nm).

from 0 to d. The ridges and substrates of the grating are made of aluminium [21]. The grating is bounded by the air, the permittivity of the air and the grooves is $\mathcal{E}_0 = 1$.

Figure 3 shows the first and zero order diffraction efficiencies under TM conditions with grating structures shown in Fig. 1. Both the zero and the first order diffraction efficiencies show periodic oscillation as functions of grating height h under arbitrary fill factor f. The locations of peak values of the first order almost overlap with the valley values of the zero order, which means that under arbitrary f, as the zero order diffraction efficiency reaches valley value, the first order always approaches the peak. It can be seen that under arbitrary f condition, the law of change curve conforms to the periodic functions (4) and (5).

The phenomena that the grating height of the first and zero order diffraction light varies periodically is caused by the phase difference $\Delta\phi$ of the two secondary coherent light source arrays. The distribution of light intensity in the light field is determined by the interference of two secondary coherent light source arrays. Changing the grating height also changes the phase difference $\Delta\phi$, and the change of the $\Delta\phi$ is the determining factor of the light intensity change, so that the diffraction efficiency of the first and zero order changes periodically. When f = 0.46, the diffraction efficiency of the zero order reaches the lowest value: 0.0010795%, while that of the first order reaches up to 44.76%. For the grating displacement sensor which uses the first order diffraction light as signal of displacement, a smaller zero order diffraction means a higher signal-to-noise ratio.

In order to more intuitively reflect the interaction between two secondary coherent light source arrays on the model, two specific grating heights were selected to observe the energy distribution of the first and zero order diffraction light. Figure 4 demonstrates the light distribution of the dual secondary coherent light source array using the finite-difference time-domain method (FDTD) [22]. The fill factor is f = 0.46 and the wavelength of the fundamental mode λ_f is 514 nm for f = 0.46. As the number of periods N covered by the incident light is limited, only 15 periods are modelled to demonstrate the light distribution of the model while reducing the computational work.

Figure 4a demonstrates that the light is mainly distributed in the first order direction for $\Delta\phi = \pi$ (corresponding to $h = \lambda_f/4 = 129$ nm) due to the constructive interference of light 1 and light 2. Meanwhile, the zero order light nearly disappears due to the destructive interference by the light 1 and light 2. Figure 4b demonstrates that the light is mainly distributed in zero order direction for $\Delta\phi = 2\pi$ (corresponding to $h = \lambda_f/2 = 257$ nm), which shows the phenomena of contrary behaviour compared to Fig. 4a. The light is mainly distributed in the zero order direction for $\Delta\phi = 2\pi$ due to the constructive interference of light 1 and light 2, meanwhile the first order light nearly disappears due to the destructive interference by the light 1 and

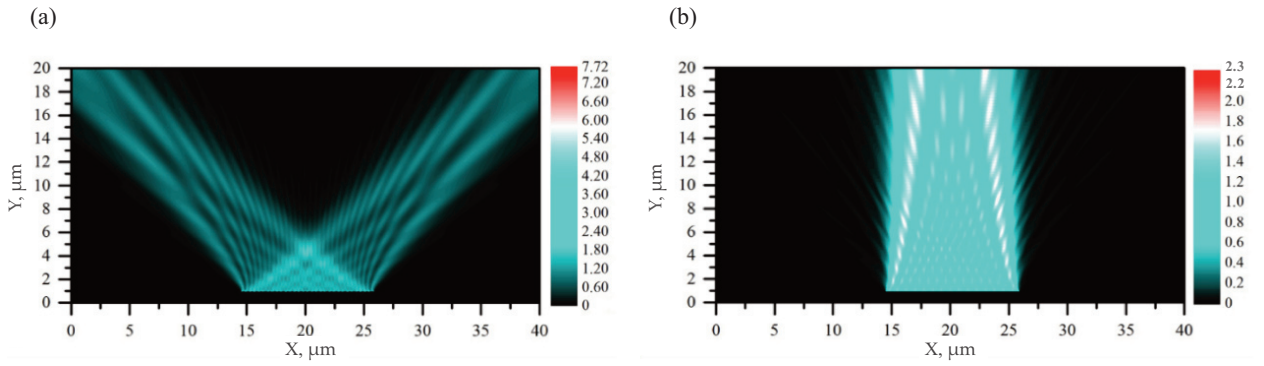

Fig. 4. Light distribution of the secondary light source 1 and the secondary light source 2 corresponding to h = 129 nm (a) and h = 257 nm (b).

light 2. When the energy of the zero order diffraction light reaches the lowest point, most of the energy of the incident light is allocated to the first order. When the energy of the first order diffracted light is the lowest, the energy of the incident light is mostly converted to zero order.

4. CONCLUSIONS

In this paper, a dual secondary coherent light source array model for TM light was proposed, and formulae for diffraction efficiency of the first and zero order diffraction light with grating height parameters were established. When the height of grating h changes while other parameters of the grating are fixed, the change of the efficiency of the first and zero order is mainly influenced by the phase difference $\Delta\phi = 4\pi h/\lambda_f$ between the two secondary light source arrays. $\Delta\phi$ depends on the propagation distance of the fundamental mode of the grating groove, which has double length of the grating height h. When $\Delta\phi$ is equal to π multiplied by any odd number (corresponding to $h = (2M+1)\lambda_f/4$), the diffraction efficiency of the first order reaches the maximum, while the diffraction efficiency of the zero order is the minimum. When $\Delta\phi$ is equal to π multiplied by any even number (corresponding to $h = M\lambda_f/2$), the diffraction efficiency of the first order reaches the minimum, while that of the zero order reaches the maximum. This means that at some specific grating height h, the phase difference $\Delta\phi$ leads to interference enhancement in direction of the first or zero order, and interference cancellation in other direction.

In addition, the periodical change of the first and the zero order diffraction efficiencies with grating height h is caused by the change of $\Delta\phi$, while the change of $\Delta\phi$ is caused by the change of the grating height. According to the above analysis, the model establishes the relationship between the law of diffraction of reflective rectangular metallic grating and the grating height. The interrelation between the zero and the first order diffraction efficiency on the grating height can also be explicated by the model. Compared to the existing diffraction theory, this model can more intuitively reflect and explain the causes of the first and the zero order diffraction efficiencies' regularity of the periodic variation with grating height, and the essential cause of the interaction between the zero and the first order diffraction light. It can also predict the diffraction efficiency of rectangular metallic grating and provide guidance for the design of rectangular metallic grating.

ACKNOWLEDGEMENTS

This work is supported by the National Natural Science Foundation of China (Nos 51675076, 51505062, 51621064). The publication costs of this article were partially covered by the Estonian Academy of Sciences.

REFERENCES

1. Ebbesen, T. W., Lezec, H. J., Ghaemi, H. F., Thio, T., and Wolff, P. A. Extraordinary optical transmission through sub-wavelength hole arrays. *Nature*, 1998, **391**, 667–669.
2. Porto, J. A., García-Vidal, F. J., and Pendry, J. B. Transmission resonances on metallic gratings with very narrow slits. *Phys. Rev. Lett.*, 1999, **83**, 2845–2848.
3. D'Aguanno, G., Mattiucci, N., Bloemer, M. J., de Ceglia., D., Vincenti, M. A., and Alù, A. Transmission resonances in plasmonic metallic gratings. *JOSA B*, 2011, **28**(2), 253–264.
4. Astilean, S., Lalanne, P., and Palamaru, M. Light transmission through metallic channels much smaller than the wavelength. *Opt. Commun.*, 2000, **175**(4–6), 265–273.
5. Chu, J., Zhang, Y., Wang, Z., and Guan, L. Polarizing color filter based on subwavelength metallic grating with grooves carved in. *Opt. Commun.*, 2014, **315**, 32–36.
6. Wang, Z., Chu, J., and Wang, Q. Transmission analysis of single layer sub-wavelength metal gratings. *Acta Optica Sinica*, 2015, **35**, 0705002(1–7).
7. Yu, Z., Liang, R., Chen, P., Huang, Q., Huang, T., and Xu, X., Integrated Tunable Optofluidics Optical Filter Based on MIM Side-Coupled-Cavity Waveguide. *Plasmonics*, 2012, **7**(4), 603–607.
8. Wang, B. and Wang, G. P. Plasmon Bragg reflectors and nanocavities on flat metallic surfaces. *Appl. Phys. Lett.*, 2005, **87**, 013107.
9. Liu, B. and Sun, Z. Plasmon resonances in deep nanogrooves of reflective metal gratings. *Photonics Nanostruct. Fundam. Appl.*, 2012, **10**(1), 119–125.
10. Cheng, F., Fei, Y.-T., and Fan, K.-C. New method on real-time signal correction and subdivision for grating-based nanometrology. In *Proceedings of the 4th International Symposium on Advanced Optical Manufacturing and Testing Technologies: Design, Manufacturing, and Testing of Micro- and Nano-Optical Devices and Systems*, Chengdu, China, November 19–21, 2008 (Han, S., Kameyama, M., and Luo, X., eds), 7284. https://doi.org/10.1117/12.832061
11. Fan, K. C., Fei, Y. T., Yu, X. F., Chen, Y. J., Wang, W. L., Chen, F., and Liu, Y. S. Development of a low-cost micro-CMM for 3D micro/nano measurements. *Meas. Sci. Technol.*, 2006, **17**(3), 524–532.
12. Fan, K. C., Liu, Y. S., Chen, Y. J., and Cheng, F. A linear diffraction grating interferometer with high accuracy. In P*roceedings of the Third International Symposium on Precision Mechanical Measurements*, *Urumqi, China, August 2–6, 2006* (Fan, K. C., Gao, W., Yu, X., Huang, W., and Hu, P., eds), 6280. https://doi.org/10.1117/12.715260
13. Ye, W., Zhang, M., Zhu, Y., Wang, L. J., Hu, J., Li, X., and Hu, C. Translational displacement computational algorithm of the grating interferometer without geometric error for the wafer stage in a photolithography scanner. *Opt. Express*, 2018, **26**(26), 34734–34752.
14. Ye, W., Zhang, M., Zhu, Y., Wang, L., Hu, J., Li, X., and Hu, C. Ultraprecision Real-Time Displacements Calculation Algorithm for the Grating Interferometer System. *Sensors*, 2019, **19**(10), 2409.
15. Hsieh, H.-L. and Pan, S.-W. Development of a grating-based interferometer for six-degree-of-freedom displacement and angle measurements. *Opt. Express*, 2015, **23**(3), 2451–2465.
16. Moharam, M. G. and Gaylord, T. K. Rigorous coupled-wave analysis of metallic surface-relief gratings. *JOSA A*. 1986, **3**(11), 1780–1787.
17. Moharam, M. G. and Gaylord, T. K. Rigorous coupled-wave analysis of planar-grating diffraction. *JOSA*, 1981, **71**, 811–818.
18. Moharam, M. G., Grann, E. B., Pommet, D. A., and Gaylord, T. K. Formulation for stable and efficient implementation of the rigorous coupled-wave analysis of binary gratings. *JOSA A*. 1995, **12**(5), 1068–1076.
19. Moharam, M. G., Pommet, D. A., Grann, E. B., and Gaylord, T. K. Stable implementation of the rigorous coupled-wave analysis for surface-relief gratings-enhanced transmittance matrix approach. *JOSA A*. 1995, **12**(5), 1077–1086.
20. Born, M. and Wolf, E. *Principles of Optics: Electromagnetic Theory of Propagation, Interference and Diffraction of Light, 7th ed*. Cambridge University Press, Cambridge, 1999.
21. Palik, E. D. *Handbook of Optical Constants of Solids*. Academic Press, Orlando, 1985.
22. Yee, K. Numerical solution of initial boundary value problems involving maxwell's equations in isotropic media. *IEEE Trans. Antennas Propag.*, 1966, **14**(3), 302–307.